Determining Ca^{2+}-sensor binding time and its variability in evoked neurotransmitter release

Ava Chomee Yoon[1], Vinnie Kathpalia[1], Sahana D'Silva[1], Aylin Cimenser[2] and Shao-Ying Hua[1]

[1]*Department of Biological Sciences, Barnard College, Columbia University, 3009 Broadway, New York, NY 10027, USA*
[2]*Center for Theoretical Neuroscience, Center for Neurobiology and Behavior, Kolb Research Annex, Columbia University, 1051 Riverside Drive, New York, NY 10032–2695, USA*

The speed and reliability of neuronal reactions are important factors for proper functioning of the nervous system. To understand how organisms use protein molecules to carry out very fast biological actions, we quantified single-molecule reaction time and its variability in synaptic transmission. From the synaptic delay of crayfish neuromuscular synapses the time for a few Ca^{2+} ions to bind with their sensors in evoked neurotransmitter release was estimated. In standard crayfish saline at room temperature, the average Ca^{2+} binding time was 0.12 ms for the first evoked quanta. At elevated extracellular Ca^{2+} concentrations this binding time reached a limit due to saturation of Ca^{2+} influx. Analysis of the synaptic delay variance at various Ca^{2+} concentrations revealed that the variability of the Ca^{2+}-sensor binding time is the major source of the temporal variability of synaptic transmission, and that the Ca^{2+}-independent molecular reactions after Ca^{2+} influx were less stochastic. The results provide insights into how organisms maximize reaction speed and reliability.

(Resubmitted 27 July 2007; accepted after revision 4 December 2007; first published online 6 December 2007)
Corresponding author S.-Y. Hua: Department of Biological Sciences, Barnard College, Columbia University, 3009 Broadway, New York, NY 10027, USA. Email: shua@smcm.edu

High-speed biological functions such as neurotransmitter exocytosis depend on fast dynamics of molecular interactions. To understand how these interactions affect the speed and reliability of synaptic transmission, we studied the reaction time of Ca^{2+}-dependent and Ca^{2+}-independent molecular reactions in the process of synaptic transmission, and to what extent the uncertainty of neurotransmitter release is due to Ca^{2+}-sensor binding and due to other protein reactions

Proteins required for evoked neurotransmitter release include at least synaptotagmin and SNARE proteins (SNARE: SNAP receptors) (Schiavo *et al.* 1992; Blasi *et al.* 1993; Littleton *et al.* 1993). Synaptotagmin acts as the major Ca^{2+} sensor in Ca^{2+} triggering of synaptic vesicle fusion (reviewed by Chapman, 2002), and the SNARE complex brings closer the membranes to be fused (Sollner *et al.* 1993; Lin & Scheller, 1997). In addition, several other proteins such as Unc proteins and complexin were also found to be necessary for neurotransmitter release (Sollner, 2003). Although the chemical features of these proteins have been well studied, due to their complex arrangement at the neurotransmitter release site, the *in vivo* reaction probabilities of the proteins are poorly understood.

In the first step of synaptic transmission, whether a primed synaptic vesicle can be released depends on the interaction of only a few Ca^{2+} ions with their sensors. The probability of Ca^{2+}-sensor reaction is particularly important for neuronal functions because the high Ca^{2+} concentration at the release site lasts for only a few milliseconds. This reaction probability may well set the speed limit of interneuronal communications and even the signal processing capacity of neural networks. Since it has not been possible to measure the early change in the free Ca^{2+} concentration at the release site ($[Ca^{2+}]_{RS}$) following an action potential, Ca^{2+}-sensor binding rate was estimated by simulating synaptic responses induced with prolonged elevation in $[Ca^{2+}]_{RS}$ (Bollmann *et al.* 2000; Schneggenburger & Neher, 2000; Millar *et al.* 2005). We realized that although it is impossible to measure the reaction time of a few molecules in most biological and chemical reaction systems, synaptic transmission is an event where the total reaction time of a few molecules in the process can be accurately determined owing to the magnification of the reaction by thousands of neurotransmitter molecules released from one synaptic vesicle. This feature of synaptic transmission allowed us to quantify the reaction time of a few molecules in physiological synaptic transmission.

Traditionally, synaptic transmission is studied from the magnitude of synaptic response. The measured total response amplitude is a nonlinear sum of quantal response

 DOI: 10.1113/jphysiol.2007.130740

amplitude, and the quantal amplitude is proportional to the product of the probabilities of all molecular reactions in synaptic transmission. Estimations of individual reaction probabilities from the total synaptic response amplitude often carry huge errors. Synaptic delay, on the contrary, is the linear sum of the Ca^{2+}-dependent and Ca^{2+}-independent reaction times; and linear summation allows more accurate estimation of individual reaction times and their variances. By analysing the variability of Ca^{2+}-dependent and Ca^{2+}-independent reaction times in synaptic transmission, we found that the uncertainty of synaptic transmission is mostly due to the Ca^{2+}-dependent molecular reactions. This indicates that most of the Ca^{2+}-independent reactions in synaptic transmission such as lipid bilayer fusion and other possible protein interactions including SNARE protein binding occur with a relatively high probability.

Methods

Neuromuscular preparation

Crayfish (*Procambarus clarkii*) of two inches were purchased from Atchafalaya Biological Supply Co. (Raceland, LA, USA), housed in fresh water at room temperature for up to 3 months and fed a diet of fish food pellets. For each experiment, one of the first pair of walking legs was quickly detached from a crayfish, partially by autotomy. Care was taken to ensure that animal discomfort was kept to a minimum. The neuromuscular preparations of leg muscle extensor were dissected from the meropodite segment in crayfish salines with different Ca^{2+} concentrations as required for electrophysiological recordings. See Hoyle & Wiersma (1958) for anatomy of the walking leg. The frozen animal tissue was destroyed by a qualified biological hazards control company.

The normal crayfish saline contained (mM): 205 NaCl, 5.4 KCl, 13.5 $CaCl_2$, 2.7 $MgCl_2$, 10 Hepes (*N*-[2-hydroxyethyl]piperazine-*N*′-[2-ethanesulphonic acid]) and 10 glucose, pH 7.39–7.41. When salines with different Ca^{2+} concentrations were used, equinormal NaCl was added or reduced to maintain the salines' osmolarity, and Mg^{2+} concentration was kept constant. For salines containing Sr^{2+}, glucose concentration was adjusted to achieve equal osmolarity for the salines.

Electrophysiology

To induce synaptic activities, the crayfish leg nerve was stimulated through a platinum wire placed close to the proximal end of the nerve. Single square pulses of 0.3 or 0.5 ms were applied at 0.1 Hz. Both the axon action potentials and muscle fibre excitatory postsynaptic potentials (EPSPs) were recorded with intracellular sharp microelectrodes filled with 3 M KCl (resistance: ∼3 MΩ) as described before (Hua & Charlton, 1999).

Single nerve terminal spikes and postsynaptic responses were recorded extracellularly with a method described by Millar *et al.* (2002). To locate the phasic nerve terminals, the preparation was incubated with 2 μM 4-(4-(diethylamino)styryl)-*N*-methylpyridinium iodide (4-Di-2-Asp; Molecular Probes, Eugene, OR, USA) in a saline for 4 min in order to visualize nerve terminals under a fluorescence microscope (modified from Olympus BX40). Micropipette electrodes (filled with a saline, resistance: ∼1.0 MΩ) were placed under a 40× water immersion objective (W.D. 3.3 mm) on single phasic terminals at an angle of about 30 deg for extracellular focal recording. The tip of the micropipettes had been ground at 30 deg using a micropipette beveller (BV-10, Sutter Instrument Co., Novato, CA, USA) to obtain an opening of 5–15 μm across, and the opening was heat polished to reduce possible damage to the preparation.

Standard preamplifiers (model 1600 of A-M Systems, Carlsborg, WA, USA) were used for both intracellular and extracellular recordings. To increase the time resolution, the low-pass filter of the amplifiers was set at 50 kHz. Tomahocq computer software (Thomas A. Goldhorpe, University of Toronto, Canada), combined with an analog/digital interface (LM-12, Dagan, Minneapolis, MN, USA), was used for data acquisition. The interface allowed a sampling rate of 100 kHz.

All the experiments were conducted at room temperature (23–25°C). To avoid incomplete change of Ca^{2+} concentration at the nerve terminals due to pipette seal, each preparation was kept only at one Ca^{2+} concentration for extracellular recordings.

Data analysis

The minimum synaptic delay was measured as the time period from the negative peak of the presynaptic spikes to the start time of the excitatory postsynaptic currents (EPSCs). Since individual nerve spikes were often too small to be measured accurately, 10 traces were averaged for the measurement of spike peaks. This average was allowed because the variation of the nerve terminal spike timing was very small compared to the synaptic delay variation. The start time of individual EPSCs and EPSP maximum derivative were determined using routines written in MATLAB (The Mathworks, Natick, MA, USA). The recordings after the stimulus were first smoothed with a median filter (temporal resolution: 0.1 ms). For recordings of EPSCs, a section of the data that was continuously below two standard deviations (∼0.1 mV) of the baseline fluctuation was extracted. The time corresponding to the beginning of the extracted data section was defined as the EPSC starting time.

Curve fitting was conducted using the nonlinear regression function of SigmaStat 3.0 (Systat Software Inc., San Jose, CA, USA). For curve fitting using the maximum derivative of EPSPs, 30 EPSPs were recorded from each muscle fibre, and the mean of the maximum derivative of all the EPSPs at the same condition was used for curve fitting.

Results

Estimating Ca^{2+} concentration at the release site

To estimate the reaction time of Ca^{2+} with its sensor in synaptic transmission, we need to know the concentration of free Ca^{2+} ions at the release site, $[Ca^{2+}]_{RS}$. Since it is impossible to directly measure the submembrane Ca^{2+} concentration for a few milliseconds immediately after an action potential, we estimated $[Ca^{2+}]_{RS}$ as a function of the extracellular Ca^{2+} concentration ($[Ca^{2+}]_o$):

$$[Ca^{2+}]_{RS} = [Ca^{2+}]_{RS\text{-}max}/(1 + K_{D\text{-}Ca}/[Ca^{2+}]_o), \quad (1)$$

where $[Ca^{2+}]_{RS\text{-}max}$ is the maximum $[Ca^{2+}]_{RS}$ which is reached when $[Ca^{2+}]_o$ is infinite and calcium influx is fully saturated, and $K_{D\text{-}Ca}$ is the $[Ca^{2+}]_o$ at which $[Ca^{2+}]_{RS}$ is half-maximal. This equation is based on the equilibrium binding reaction between Ca^{2+} ions and Ca^{2+} channels. The $K_{D\text{-}Ca}$ for Ca^{2+} influx has been estimated for several types of neurons (Akaike *et al.* 1978; Carbone & Lux, 1987). Assuming that neurotransmitter release is triggered by the binding of n Ca^{2+} ions with their sensors, synaptic responses at low Ca^{2+} influx are proportional to $([Ca^{2+}]_{RS})^n$. The synaptic response, R, at a given $[Ca^{2+}]_o$ can be expressed as:

$$\begin{aligned} R &= \beta([Ca^{2+}]_{RS})^n \\ &= \beta([Ca^{2+}]_{RS\text{-}max}/(1+K_{D\text{-}Ca}/[Ca^{2+}]_o))^n, \end{aligned} \quad (2)$$

where β is a constant; $\beta([Ca^{2+}]_{RS\text{-}max})^n$ is the maximum synaptic response (R_{max}) which is achieved when $[Ca^{2+}]_o$ is infinite. A similar version of eqn (2) was introduced by Dudel (1981). This equation provides a means to estimate the value of $K_{D\text{-}Ca}$ from the synaptic responses at various $[Ca^{2+}]_o$. Later we used $K_{D\text{-}Ca}$ to estimate Ca^{2+}-sensor binding time (see the next section of Results).

We first tested the synaptic responses of the extensor muscle fibres at various $[Ca^{2+}]_o$. Each muscle fibre of the extensor is innervated by two excitatory axons: the phasic and tonic axons (both shown in Fig. 1*A*). At low-frequency stimulation, the neurotransmitter release probability of the phasic terminals is much higher than that of the tonic terminals (Msghina *et al.* 1998); therefore the EPSPs induced at 0.1 Hz were caused by glutamate released from the phasic terminals (see Hua *et al.* 2007 for further verifications). To minimize the error in $K_{D\text{-}Ca}$ estimation due to nonlinear summation of the postsynaptic responses and the saturation of Ca^{2+} sensor and neurotransmitter receptors, the maximum derivative of the EPSPs was measured instead of EPSP amplitude to quantify the synaptic responses. At $[Ca^{2+}]_o$ ranging from 1.7 mM to 20.3 mM, the EPSP maximum derivative increased with increasing $[Ca^{2+}]_o$ (Fig. 1*D*). Intracellular recordings showed no significant effect of changes in $[Ca^{2+}]_o$ on action potentials of the phasic axon. Examples of the phasic axon action potentials and muscle fibre EPSPs at 1.7 mM and 20.3 mM $[Ca^{2+}]_o$ were shown in Fig. 1*B* and *C*, respectively (5 experiments for $[Ca^{2+}]_o$ of 1.7, 6.8 (not shown) and 20.3 mM each). After recording synaptic responses at eight $[Ca^{2+}]_o$ values, the value of $K_{D\text{-}Ca}$ was estimated by fitting eqn (2) to the mean EPSP maximum derivative at each $[Ca^{2+}]_o$. Figure 1*D* shows the mean synaptic responses and the best-fit curve with a $K_{D\text{-}Ca}$ of 5.8 mM (S.E.M. of estimation: 2.4 mM, with 2.7 mM Mg^{2+}). This value is within the range of Ca^{2+} dissociation constants for neuronal Ca^{2+} channels (2–10 mM at various $[Mg^{2+}]$: Carbone & Lux, 1987; Akaike *et al.* 1989; Aibara *et al.* 1992; Church & Stanley, 1996; Schneggenburger *et al.* 1999; Foster *et al.* 2002).

Equation (2) requires that the Ca^{2+} sensors and postsynaptic neurotransmitter receptors are not saturated at the maximum derivative of EPSPs. These saturations have been observed at some mammalian neuronal synapses (Foster *et al.* 2002). The synaptic response curve in Fig. 1*D* shows that the synaptic responses saturated at a higher level of $[Ca^{2+}]_o$. This saturation has three possible components: the saturations of Ca^{2+} influx, Ca^{2+} sensor and postsynaptic neurotransmitter receptors. In addition, saturation of intracellular Ca^{2+} buffer may add an opposite effect on the synaptic response. If the Ca^{2+} sensors or postsynaptic neurotransmitter receptors were saturated when the synapses generated their maximum derivative of EPSPs, the estimated $K_{D\text{-}Ca}$ value would not reflect the half-maximal $[Ca^{2+}]_{RS}$ correctly. We explored the significance of the saturation of Ca^{2+} sensors and neurotransmitter receptors by reducing Ca^{2+} influx. Several divalent cations are known to compete with Ca^{2+} for interaction with Ca^{2+} channels (reviewed by Hagiwara & Byerly, 1981). Among these ions, Sr^{2+} causes little synaptic response in our preparation. Therefore we used Sr^{2+} to reduce Ca^{2+} influx induced by single action potentials. The $[Ca^{2+}]_{RS}$ in the presence of Ca^{2+} and Sr^{2+} can be calculated as:

$$\begin{aligned} [Ca^{2+}]_{RS} = [Ca^{2+}]_{RS\text{-}max}\,(1+K_{D\text{-}Ca}(1 + [Sr^{2+}]_o \\ /K_{D\text{-}Sr})/[Ca^{2+}]_o), \end{aligned} \quad (3)$$

where K_{D-Sr} is the dissociation constant of Sr^{2+} for Ca^{2+} channels. From eqns (2) and (3), the synaptic response in

the presence of Sr^{2+}, denoted as R_{Sr}, is expressed as:

$$R_{Sr} = R_{max}/(1 + K_{D\text{-}Ca}(1 + [Sr^{2+}]_o/K_{D\text{-}Sr})/[Ca^{2+}]_o)^n, \quad (4)$$

where R_{max} is the maximum synaptic response. If the saturation of the synaptic response shown in Fig. 1*D* was solely due to the saturation of Ca^{2+} influx, reducing Ca^{2+} influx by adding Sr^{2+} should not change the value of estimated $K_{D\text{-}Ca}$. But if the saturation of the synaptic response was largely due to the saturation of Ca^{2+} sensors or postsynaptic receptors, reducing Ca^{2+} influx by adding Sr^{2+} would reduce the saturation of the sensors or receptors, thus leading to a larger $K_{D\text{-}Ca}$ as estimated with eqn (4). We then tested $K_{D\text{-}Ca}$ in the presence of Sr^{2+}.

Replacing Ca^{2+} with 10 mM Sr^{2+} blocked synaptic responses (example shown in Fig. 2*A*). In four experiments, the EPSP amplitude with 10 mM Sr^{2+} and without Ca^{2+} was 0.39 ± 0.07 mV, which is very close to the amplitude in Ca^{2+}-free saline without Sr^{2+} (0.38 ± 0.11 mV, mean ± S.D.). This observation

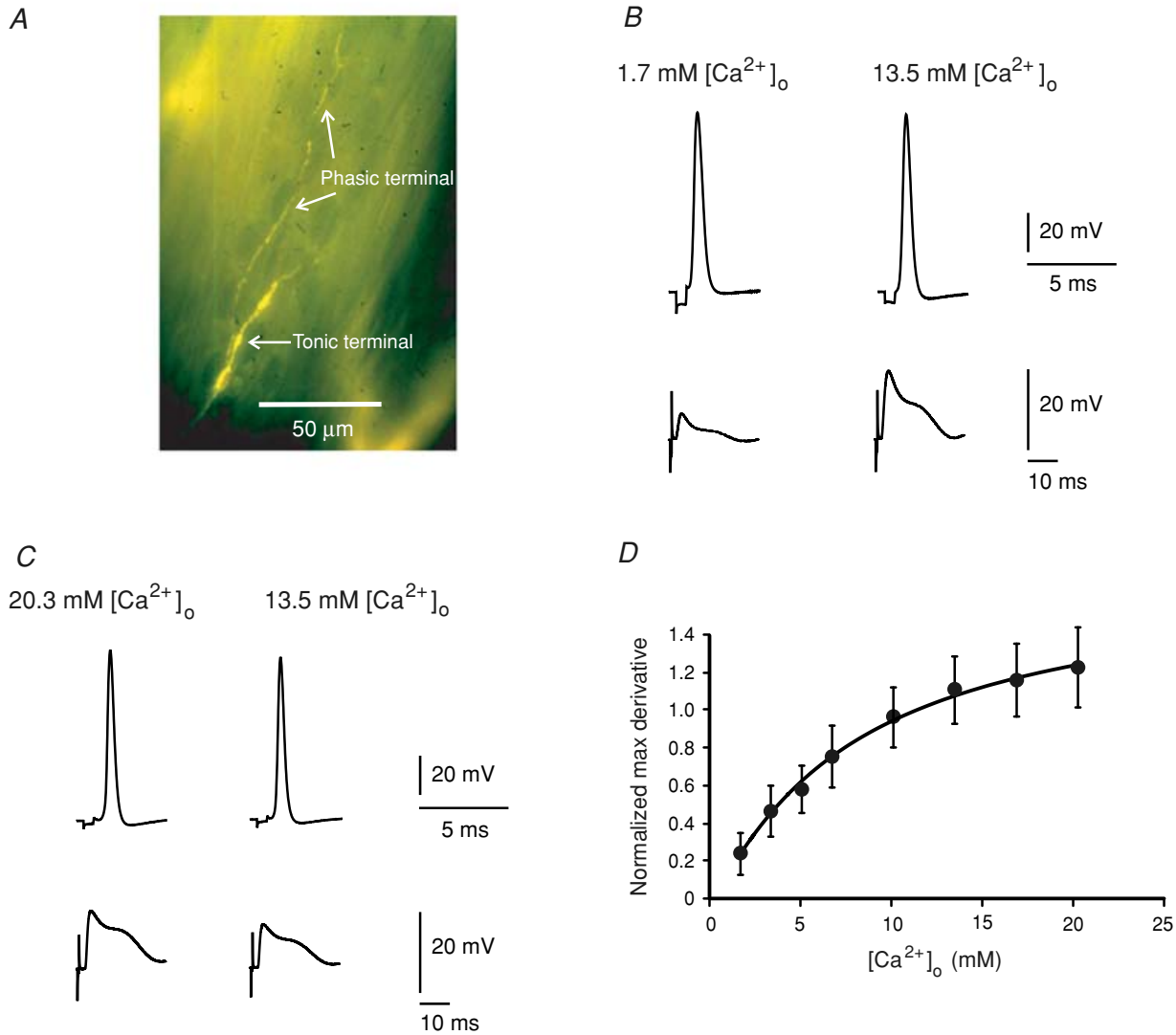

Figure 1. Intracellular recordings of the activities of crayfish motor axons and muscle fibres
A, fluorescence image of the phasic and tonic nerve terminals on an extensor muscle fibre (the image is shown in colour in the online version of this paper). *B*, action potentials of the phasic axon and EPSPs at 1.7 and 13.5 mM $[Ca^{2+}]_o$. *C*, action potentials of the phasic axon and EPSPs at 20.3 mM and 13.5 mM $[Ca^{2+}]_o$. Recordings in *B* and *C* were from different preparations. Recordings at 13.5 mM $[Ca^{2+}]_o$ were taken from the same axon and muscle fibre after the recordings at 1.7 mM or 20.3 mM $[Ca^{2+}]_o$. *D*, the synaptic responses at various $[Ca^{2+}]_o$. The mean maximum derivative of EPSPs (max derivative) was normalized to that in normal crayfish saline. For calibration the recordings in normal saline were also taken after each preparation was thoroughly washed in normal crayfish saline. Data were from five preparations for each $[Ca^{2+}]_o$. Error bars show the S.D. The line is the best fit of eqn (2) to the mean maximum derivative.

confirmed that Sr^{2+} barely causes any synaptic response following low-frequency nerve stimulation. We next examined the effect of Sr^{2+} on Ca^{2+}-dependent synaptic transmission by measuring synaptic responses with and without $[Sr^{2+}]_o$. This test was repeated at different $[Ca^{2+}]_o$, for each of which the ratio of $[Sr^{2+}]_o/[Ca^{2+}]_o$ was fixed at 3/13.5. The synaptic responses measured as EPSP maximum derivative were inhibited most (by 26%) at 20.3 mM $[Ca^{2+}]_o$. The inhibition of synaptic responses by Sr^{2+} is shown in Fig. 2*B* and plotted in Fig. 2*C*. From eqns (2) and (4), this inhibition can be predicted as:

$$R_{Sr}/R = (1 + K_{D\text{-}Ca}/[Ca^{2+}]_o)^n/(1+K_{D\text{-}Ca}(1 + [Sr^{2+}]_o /K_{D\text{-}Sr})/[Ca^{2+}]_o)^n. \quad (5)$$

Equations (4) and (5) share parameters of $K_{D\text{-}Ca}$, $K_{D\text{-}Sr}$ and n. By multiple-function curve fitting of the two equations to the mean synaptic responses plotted in Fig. 2*C* and *D* (with $K_{D\text{-}Ca}$, $K_{D\text{-}Sr}$ and n shared for the two equations), $K_{D\text{-}Ca}$ was estimated to be 6.0 mM (S.E.M. of estimation: 3.2 mM). This value is very close to the $K_{D\text{-}Ca}$ estimated without Sr^{2+} (5.8 mM), indicating little saturation of Ca^{2+} sensor and/or postsynaptic receptors at the maximum derivative of EPSPs; therefore the $K_{D\text{-}Ca}$ reflects the feature of Ca^{2+} influx.

Determining mean time for Ca^{2+}-sensor binding

With the estimated $K_{D\text{-}Ca}$ value, we next estimated the Ca^{2+}-dependent molecular reaction time in synaptic

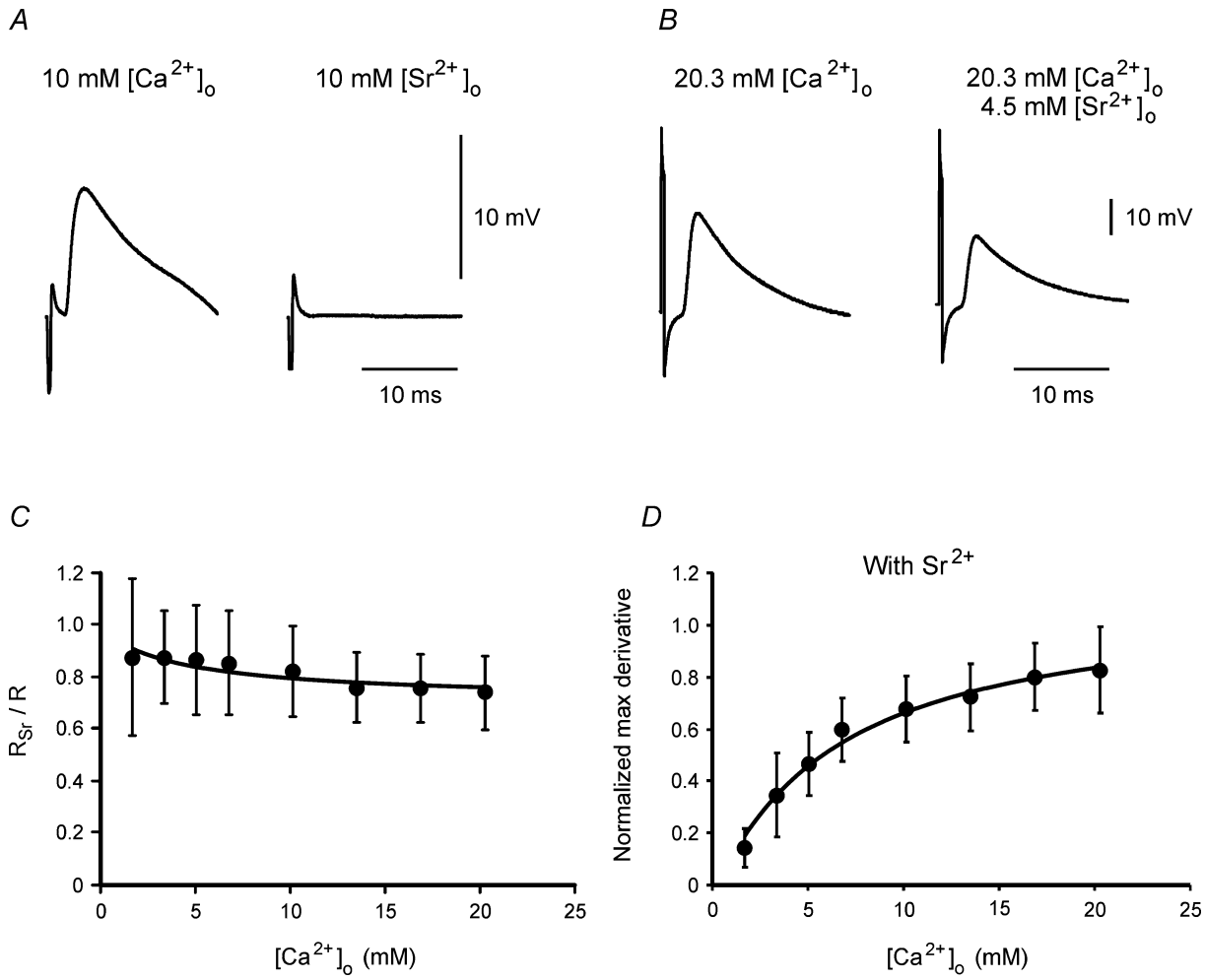

Figure 2. Synaptic responses in the presence of Sr^{2+}
A, synaptic responses in saline of 10 mM Ca^{2+} and saline of 10 mM Sr^{2+}. The recordings were from the same muscle fibre. *B*, Sr^{2+} inhibits synaptic transmission. The recordings were from the same muscle fibre. In *A* and *B*, the axon was stimulated at 0.1 Hz and each trace is an average of 5 recordings. *C*, inhibition of synaptic response by Sr^{2+} at various $[Ca^{2+}]_o$. The ratio of the EPSP maximum derivative in the presence of Sr^{2+} (R_{Sr}) to that in salines without Sr^{2+} (R) was plotted to $[Ca^{2+}]_o$. The line is the best fit of eqn (5). *D*, synaptic responses at various $[Ca^{2+}]_o$ and $[Sr^{2+}]_o$. The EPSP maximum derivatives were normalized to that in saline of 13.5 mM Ca^{2+} (without Sr^{2+}). The line is the best fit of eqn (4). In *C* and *D*, concentrations of $[Sr^{2+}]_o$ are 3/13.5 times $[Ca^{2+}]_o$ for each saline; data are means of 5–7 experiments for each $[Ca^{2+}]_o$ and errors are S.D.

transmission from the minimum synaptic delays at various $[Ca^{2+}]_o$. Synaptic activities were recorded extracellularly by placing pipette electrodes on single phasic nerve terminals. Following each stimulus, a presynaptic current and an excitatory postsynaptic current (EPSC) were detected as voltage signals (shown in Figs 3*A* and 4*A*). When the axon was stimulated at 0.1 Hz, the minimum synaptic delay, which was the delay of the first quantum, was stable for the period of experiments as long as $[Ca^{2+}]_o$ was not changed. In normal crayfish saline, the minimum synaptic delay of 15 single terminals from 10 preparations was 0.61 ± 0.13 ms (mean ± s.d.), which was comparable to the synaptic delays for other types of synapses (Katz & Miledi, 1965; Llinás *et al.* 1981; Sabatini & Regehr, 1996; Waldeck *et al.* 2000).

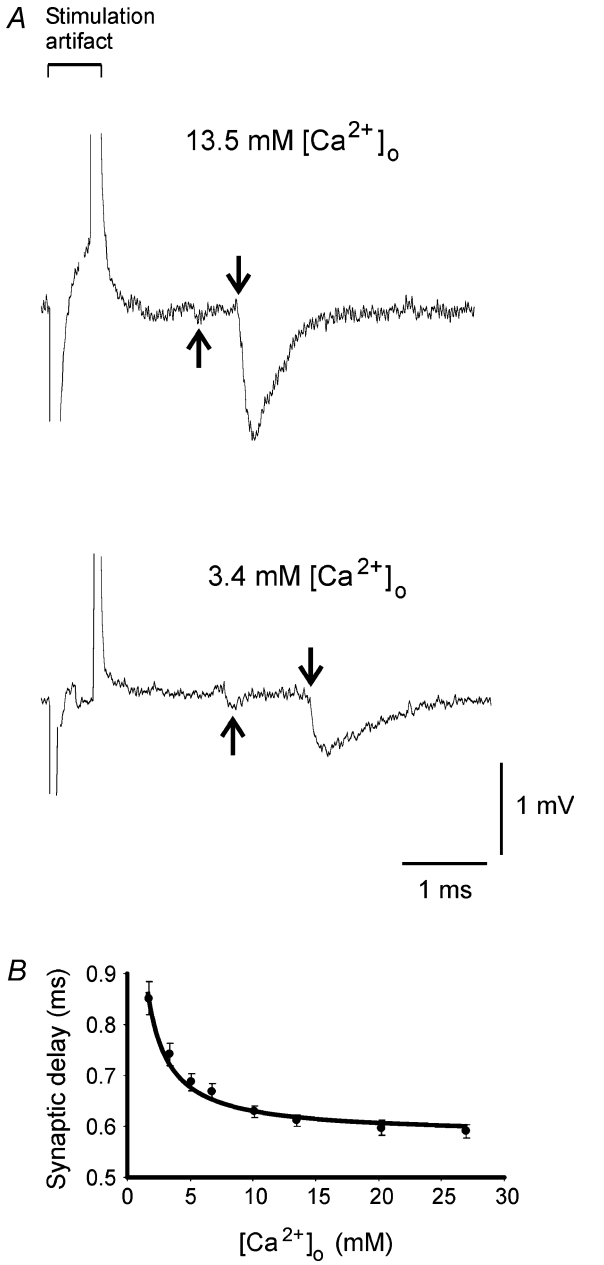

Figure 3. The synaptic delay is Ca^{2+} dependent
A, the nerve terminal spikes and postsynaptic responses at $[Ca^{2+}]_o$ of 13.5 mM and 3.4 mM as labelled. The arrows point to the negative peak of the nerve terminal spikes and the onset of the postsynaptic responses. The large noise of the recordings was due to 50 kHz low-pass filter used for recording. *B*, mean synaptic delays at various $[Ca^{2+}]_o$. Data were collected from 10–15 single nerve terminals for each $[Ca^{2+}]_o$. Errors are S.E.M. The curve is the best fit of eqn (9) to the mean synaptic delays.

Synaptic responses were then induced in eight salines differing in $[Ca^{2+}]_o$, and synaptic delays were measured. The presynaptic signal and EPSCs at two Ca^{2+} concentrations are shown in Fig. 3*A*. The minimum synaptic delay at eight $[Ca^{2+}]_o$ values (plotted in Fig. 3*B*) revealed that the synaptic delay was $[Ca^{2+}]_o$ dependent, with longer delay at lower Ca^{2+} concentrations, and that the delay approached a steady level at high $[Ca^{2+}]_o$. These features allowed us to analyse Ca^{2+}-dependent and Ca^{2+}-independent components of the minimum synaptic delay.

The synaptic delay is the total time for the following events in series: Ca^{2+} channel opening, Ca^{2+} influx and Ca^{2+}-sensor binding, the possible SNARE protein interaction and other molecular reactions not well-defined yet, lipid membrane fusion, neurotransmitter release and diffusion, and postsynaptic response generation. The synaptic delay and its variance were mainly attributed to presynaptic events, since neurotransmitter diffusion across the synaptic cleft and postsynaptic events take little time (Katz & Miledi, 1965). Among the presynaptic events, the rates of Ca^{2+} influx and Ca^{2+}-sensor binding are $[Ca^{2+}]_o$ dependent. Since $[Ca^{2+}]_o$ is much higher than $[Ca^{2+}]_{RS}$, the Ca^{2+}-channel interaction takes much less time than Ca^{2+}-sensor interaction; therefore the Ca^{2+}-dependent portion of the synaptic delay is approximately the Ca^{2+} sensor binding time. For a first-order reaction with respect to Ca^{2+} binding site, the probability of the time length from Ca^{2+} influx to Ca^{2+}-sensor binding is exponentially distributed with the mean time length, t, and this time length is the inverse of the product of the binding rate constant and Ca^{2+} concentration (Colquhoun, 1971*b*). Thus the mean time required for the binding of Ca^{2+} to Ca^{2+} sensor is expressed by the equation:

$$t = 1/(k[Ca^{2+}]_{RS}), \quad (6)$$

where k is the binding rate constant. If the quantal release requires multiple Ca^{2+}-sensor binding reactions that do not overlap in time and if no unbinding occurs before the subsequent event in vesicle fusion, the total Ca^{2+}-sensor

binding time can be calculated as:

$$d - c = 1/(Nk[Ca^{2+}]_{RS}) + 1/((N-1)k[Ca^{2+}]_{RS}) + 1/((N-2)k[Ca^{2+}]_{RS}) + \ldots + 1/((N-N+1)k[Ca^{2+}]_{RS}), \quad (7)$$

where d denotes the minimum synaptic delay, c is the time for all the Ca^{2+}-independent reactions in synaptic transmission, and N is the number of the binding sites required for one vesicle fusion. The unbinding rate of the Ca^{2+} sensor was not included in eqn (7) because the unbinding rate for the putative Ca^{2+} sensor in neurotransmitter release was estimated to be low (Bollmann *et al.* 2000) relative to our estimated Ca^{2+}-sensor binding time, and only the vesicles that experienced no Ca^{2+} unbinding have a high probability to be released first after each nerve terminal spike. The minimum synaptic delay we measured was the delay of these vesicles.

Combining eqns (1) and (7) we have the equation for synaptic delay:

$$d = c + (\gamma/(k[Ca^{2+}]_{RS\text{-}max})) \times (1 + K_{D\text{-}Ca}/[Ca^{2+}]_o), \quad (8)$$

where $\gamma \equiv 1/N + 1/(N-1) + 1/(N-2) + \ldots + 1/(N-N+1)$.

Let $e_1 = c + \gamma/(k[Ca^{2+}]_{RS\text{-}max})$, and $e_2 = \gamma K_{D\text{-}Ca}/(k[Ca^{2+}]_{RS\text{-}max})$, eqn (8) can be simplified into:

$$d = e_1 + e_2/[Ca^{2+}]_o. \quad (9)$$

Equation (9) was then fitted to the mean minimum synaptic delay at each $[Ca^{2+}]_o$ (Fig. 3*B*); the best fits of e_1 and e_2 are 0.58 ms (S.E.M. 0.01 ms) and 0.47 ms mM (S.E.M. 0.03 ms mM), respectively. From e_1, e_2 and $K_{D\text{-}Ca} = 5.8$ mM, the Ca^{2+}-independent portion of the minimum synaptic delay, c, was calculated to be 0.50 ms ($c = e_1 - e_2/K_{D\text{-}Ca}$). The estimate of c carries errors of e_1, e_2 and $K_{D\text{-}Ca}$. From these errors, we estimated the S.E.M. of c to be less than 0.03 ms.

From eqn (9), e_1 is the minimum synaptic delay when Ca^{2+} current is saturated at infinite $[Ca^{2+}]_o$, and is the lower limit of the synaptic delay at a particular temperature. The value of e_2 is a constant for $[Ca^{2+}]_o$-dependent change in synaptic delay. With these two parameters, the minimum synaptic delay can be calculated if one knows $[Ca^{2+}]_o$ ($d = 0.58$ ms $+ 0.47$ ms mM$/[Ca^{2+}]_o$). From eqns (8) and (9), the ratio of e_2 over $K_{D\text{-}Ca}$ ($= \gamma/(k[Ca^{2+}]_{RS\text{-}max})$) denotes another constant (0.08 ms, S.E.M.: 0.03 ms), which is the Ca^{2+}-sensor binding time at $[Ca^{2+}]_{RS\text{-}max}$ (see eqn (6) for the binding time). Thus the synaptic delay can also be calculated as 0.50 ms $+ 0.08$ ms $\times (1 + K_{D\text{-}Ca}/[Ca^{2+}]_o)$.

Once we know the Ca^{2+}-independet reaction time, how long it takes for a single Ca^{2+} ion to bind to a binding site can be calculated if we know how many Ca^{2+} ions are required for one quantum and whether they bind with the sensors simultaneously or in series. Since Dodge & Rahamimoff (1967) proposed that $\sim$4 Ca^{2+} ions were required for each quantum, experimental findings suggested that 1–5 Ca^{2+} ions are required to release 1 vesicle of neurotransmitter (Llinás *et al.* 1976; Charlton *et al.* 1982; Zucker & Stockbridge, 1983; Bollmann *et al.* 2000; Schneggenburger & Neher, 2000). In normal crayfish saline, if only 1 Ca^{2+} is required for a quantum, the binding time calculated from eqn (8) is 0.12 ms. If, on the other hand, 5 Ca^{2+} ions are required to bind with their identical sensors in sequence, the individual Ca^{2+}-sensor binding time is 0.05 ms. If each binding increases the subsequent binding affinity, or the binding times overlap, each binding should take 0.05–0.12 ms.

Using minimum synaptic delay measurements, we also examined the delay distribution of the first quantal event after nerve spikes. At all the Ca^{2+} concentrations tested, single action potentials often caused multiple quanta from single phasic nerve terminals, but most of the quanta were relatively synchronized (see Fig. 4*A*). The delay distribution of EPSCs induced with 50 stimuli at 0.1 Hz (6 failures; $[Ca^{2+}]_o$: 16.9 mM; examples shown in Fig. 4*A*) is shown in Fig. 4*B*, and these EPSCs were summed to construct a compound EPSC (Fig. 4*C*) illustrating an EPSC of a muscle fibre with 50 phasic terminals. The distribution of the minimum synaptic delay showed that the single terminal EPSCs started during the period from the onset to the negative peak of the compound EPSC. This distribution was common at various $[Ca^{2+}]_o$. This means that the first quanta we analysed occurred up to the negative peak of the compound EPSC. These first quanta should result from the exocytosis of the vesicles that are relatively homogeneous in their priming status and their access to Ca^{2+} source. In our estimation of the Ca^{2+}-independent component of synaptic delay, we assumed that $[Ca^{2+}]_{RS}$ is constant during Ca^{2+} channel opening and is very low before channel opening and after channel closing. This assumption is based on findings of simulation studies that in the vicinity of Ca^{2+} channels, $[Ca^{2+}]_{RS}$ reaches a steady level in a few microseconds after channel opening and reduces quickly when the channel closes (Simon & Llinás, 1985; Shahrezaei & Delaney, 2004). Consistent with this notion, the frequency of the first quanta increased promptly after a short period following the nerve spike and most of the first quanta occurred during a period of 400 μs in Fig. 4.

Determining synaptic delay variance

The synaptic delay of the phasic synapses had a considerable variance. This can be seen from Fig. 5*A*, which shows EPSCs induced with five consecutive stimuli of 0.1 Hz in normal crayfish saline. The variance was

even larger at lower $[Ca^{2+}]_o$. Studies on frog neuromuscular synapses suggested that the variance of synaptic delay reflects a presynaptic probabilistic process (Barrett & Stevens, 1972). We wanted to know to what extent the variance was associated with Ca^{2+}-sensor binding. Since the minimum synaptic delay was caused by two types of non-overlapping processes: the Ca^{2+}-dependent and Ca^{2+}-independent reactions, the variance of the minimum synaptic delay should be the sum of the variances of the two processes. From eqn (8) the variance of the minimum synaptic delay (see Colquhoun, 1971*a*) is:

$$\mathrm{var}(d) = \mathrm{var}(c) + \mathrm{var}(\gamma/(k[Ca^{2+}]_{RS\text{-}max})) \times (1+K_{D\text{-}Ca}/[Ca^{2+}]_o)^2, \quad (10)$$

in which $\mathrm{var}(c)$ and $\mathrm{var}(\gamma/(k[Ca^{2+}]_{RS\text{-}max})) \times (1 + K_{D\text{-}Ca}/[Ca^{2+}]_o)^2$ are the variances of $[Ca^{2+}]_o$-independent and $[Ca^{2+}]_o$-dependent portions of the synaptic delay, respectively. In eqn (10), $K_{D\text{-}Ca}$ is a constant and $[Ca^{2+}]_o$ does not change for a particular saline. Because Ca^{2+}-sensor binding carries considerable uncertainty, k is the major source of the variance. Whether γ changes from trial to trial is not known. Therefore γ is treated as a possible source of variance. The variance of the minimum synaptic delay ($\mathrm{var}(d)$) was calculated for each $[Ca^{2+}]_o$ and plotted in Fig. 5*B*. By fitting eqn (10) to the means of the variances, the variance of the Ca^{2+}-independent portion of the synaptic

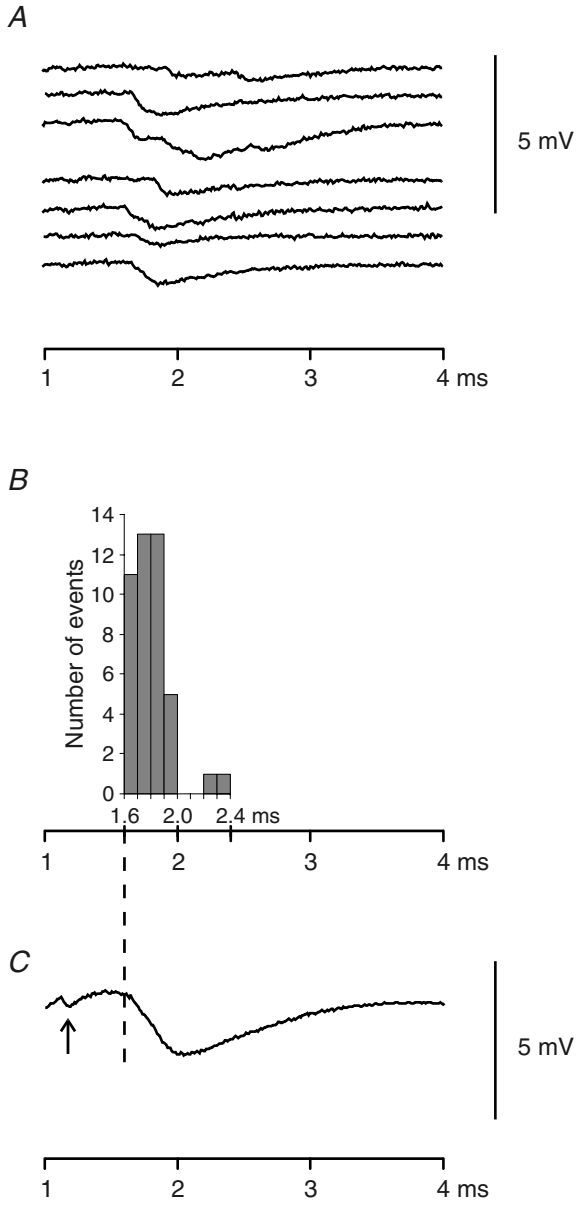

Figure 4. The temporal distribution of the first quantum delay
A, EPSCs induced with 7 stimuli at 0.1 Hz from the same location on a muscle fibre. The stimuli were applied at 0.1 ms and recordings were taken at 1.0 ms. *B*, distribution of the first quantum starting time. All the 44 EPSCs induced with 50 stimuli (at 0.1 Hz) were included. Examples of EPSCs were shown in *A*. *C*, the compound EPSC of 44 EPSCs in *B*. The arrow points to the nerve terminal spike. The time scale is the same for *B* and *C* for comparison.

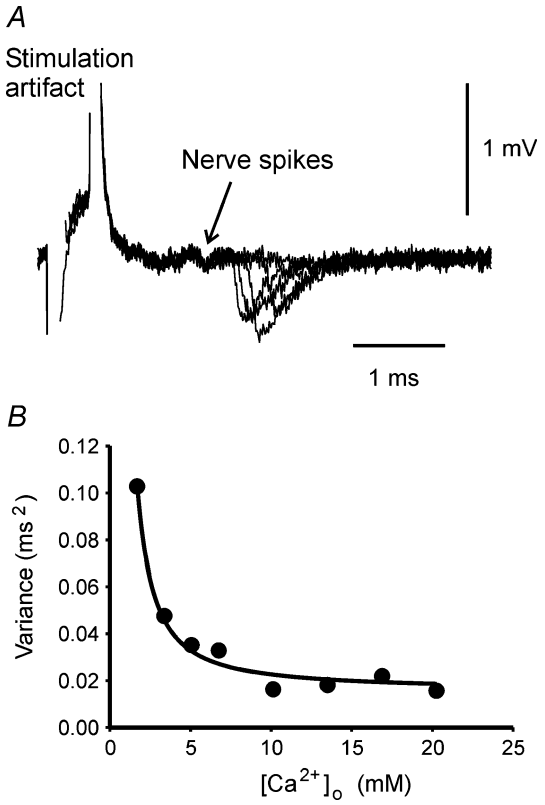

Figure 5. The variance of the synaptic delay
A, five recordings from a phasic nerve terminal and the postsynaptic fibre in normal saline were superimposed and aligned at the stimulation artifact. The synaptic delay has a large variance (with one failure). The nerve spikes prior to the synaptic responses showed little variance. *B*, the variance of the synaptic delay is Ca^{2+} dependent. The variance of the minimum synaptic delay from 10–14 muscle fibres at each Ca^{2+} concentration is plotted. The curve is the best fit of eqn (10) to the variance.

delay was estimated to be 0.011 ms^2 (S.E.M. of estimation: 0.002 ms^2). Figure 5*B* shows the curve fitting to the experimental data.

The variance of the Ca^{2+}-sensor binding time now can be calculated form eqn (10). In normal crayfish saline, the calculated total variance of minimum synaptic delay was 0.021 ms^2, meaning that 0.010 ms^2, or 48% of the delay variance, was from Ca^{2+}-sensor binding. At 1.7 mM $[Ca^{2+}]_o$, the variance of the Ca^{2+} sensor binding time was 89% of the total delay variance. The large variance of Ca^{2+}-sensor binding time is consistent with the probabilistic feature of Ca^{2+} binding with its sensor. If the Ca^{2+}-sensor binding is close to a diffusion-controlled reaction as *in vitro* (Millet *et al.* 2002), a major source of this variance should be the random walk of Ca^{2+} ions.

Discussion

Although it has been shown that synaptic delay is Ca^{2+}-influx dependent for mammalian neuronal synapses (Sabatini & Regehr, 1996; Bollmann *et al.* 2000; Schneggenburger & Neher, 2000), the synaptic delays of some neuromuscular junctions of both mammals and crustaceans are known to be Ca^{2+} independent (Datyner & Gage, 1980; Parnas *et al.* 1989; Dudel *et al.* 1991). In this study, we found that the delay is Ca^{2+} dependent at crayfish phasic neuromuscular junctions. This discrepancy may be attributed to the difference in the synapses and the range of $[Ca^{2+}]_o$ tested. The crayfish phasic neuromuscular synapses have a very high release probability which allowed us to measure the synaptic delay over a wide range of $[Ca^{2+}]_o$.

In this study, we estimated Ca^{2+}-sensor binding time from the synaptic delay of the first quanta in synaptic transmission. The synaptic vesicles that gave rise to these first quanta should be relatively uniform in their molecular arrangement for fusion. The analysis and conclusions of this study should apply only to these vesicles, which are probably already docked (or very close) to Ca^{2+} channels at the moment of Ca^{2+} channel opening. This docking is made possible by syntaxin, a protein integrated to the nerve terminal membrane. Syntaxin interacts with both Ca^{2+} channels (Bezprozvanny *et al.* 1995) and the vesicle associated membrane protein (VAMP, synaptobrevin). Due to this docking, the minimum distance between a vesicle and a Ca^{2+} channel has been estimated to be less than 20 nm (Shahrezaei & Delaney, 2004). Equation (8) cannot be used for vesicles with various distances from Ca^{2+} channels: the reaction time of Ca^{2+}-sensor binding for these vesicles highly depends on the distances between the vesicles and Ca^{2+} channels, and the synaptic delay for these vesicles would more likely be affected by Ca^{2+} unbinding rate.

The challenge in estimating molecular reaction times and variances is to reduce unknown factors in the process so that the estimates are relatively accurate. We strived to reduce the number of free parameters in curve fitting. In the equation for Ca^{2+}-sensor binding time we have only two unknown parameters (see eqn (9)). This equation provided a unique set of estimates with reasonable estimation errors. Other factors related to estimation error are discussed as follows. Synaptic vesicle fusion is believed to be caused by multiple Ca^{2+} bindings, but it is not known whether all the binding sites bind with Ca^{2+} with the same probability. Our method does not assume a fixed binding probability for all the binding sites, and the cooperativity of Ca^{2+}-sensor binding does not affect the accuracy of the estimations of the total Ca^{2+}-binding time. With our approach, the value of $K_{D\text{-}Ca}$ for $[Ca^{2+}]_o$–$[Ca^{2+}]_{RS}$ conversion was estimated from synaptic responses, and therefore the Ca^{2+} influx that was not related to neurotransmitter release was not included. The major error source for our estimation resides in the estimation of $K_{D\text{-}Ca}$ value. With three free parameters in eqn (2), the estimation of $K_{D\text{-}Ca}$ has a relatively large error. Another possible source of estimation error is the assumption that $[Ca^{2+}]_{RS}$ is constant during Ca^{2+}-sensor reaction. If more than one Ca^{2+} channel contributes to the fusion of the same vesicle, $[Ca^{2+}]_{RS}$ cannot be a constant value for Ca^{2+} sensor binding. However, this assumption affects $[Ca^{2+}]_{RS}$ estimations at all Ca^{2+} concentrations to a similar extent, and therefore would not affect the main conclusions of this study. Lastly, the assumption that no unbinding occurs for the first quanta may affect the accuracy of the estimation.

The length and variance of the Ca^{2+}-independent reaction time in synaptic transmission reflect the overall reaction probability of several proteins and lipid molecules involved in synaptic transmission. A simulation model by Schneggenburger & Neher (2000) provided a lower limit estimate of the rate constant for the Ca^{2+}-independent events in vesicle fusion (6000 s^{-1}, mammalian neurons). With our method, these events take 0.50 ± 0.03 ms in normal saline. While this 0.5 ms accounts for 81% of the total synaptic delay for the first quanta in normal crayfish saline, the variance of these reactions is only 52% of the total delay variance. The low variability of the Ca^{2+}-independent reaction time is important for reliability of synaptic transmission. Indeed, neurons cannot afford a large number of stochastic processes in synaptic transmission. The release machinery and the structure of lipid bilayer are believed to be very similar between crustaceans and mammals. For both, the Ca^{2+}-independent portion of the synaptic delay is composed of the time for Ca^{2+} channels to open, the time for Ca^{2+} and molecular machinery to cause vesicle fusion with the nerve terminal membrane, the subsequent neurotransmitter release and the brief time for generation of the postsynaptic response. Among these events, Ca^{2+}

channel opening is known to be a probabilistic process; the variability of the timing of channel opening should contribute substantially to the synaptic delay variance. This leaves very little variance for other protein reactions including SNARE complex formation. Therefore, the stochastic feature of the vesicular release cannot be explained with SNARE protein interactions. Furthermore, the best way to achieve a low variability of reaction time is to keep the proteins that interact following Ca^{2+}-sensor binding very close but separated from each other before Ca^{2+} influx. This idea has been expressed in a model of partial SNARE complex (Hua & Charlton, 1999) combined with a negative switch in vesicle fusion (Hua *et al.* 2007). The model allows very short synaptic delay and low variability of Ca^{2+}-independent protein reactions in synaptic transmission.

References

Aibara K, Ebihara S & Akaike N (1992). Voltage-dependent ionic currents in dissociated paratracheal ganglion cells of the rat. *J Physiol* **457**, 591–610.

Akaike N, Kostyuk PG & Osipchuk YV (1989). Dihydropyridine-sensitive low-threshold calcium channels in isolated rat hypothalamic neurones. *J Physiol* **412**, 181–195.

Akaike N, Lee KS & Brown AM (1978). The calcium current of Helix neuron. *J Gen Physiol* **71**, 509–531.

Barrett EF & Stevens CF (1972). The kinetics of transmitter release at the frog neuromuscular junction. *J Physiol* **227**, 691–708.

Bezprozvanny I, Scheller RH & Tsien RW (1995). Functional impact of syntaxin on gating of N-type and Q-type calcium channels. *Nature* **378**, 623–626.

Blasi J, Chapman ER, Yamasaki S, Binz T, Niemann H & Jahn R (1993). Botulinum neurotoxin C1 blocks neurotransmitter release by means of cleaving HPC-1/syntaxin. *EMBO J* **12**, 4821–4828.

Bollmann JH, Sakmann B & Borst JG (2000). Calcium sensitivity of glutamate release in a calyx-type terminal. *Science* **289**, 953–957.

Carbone E & Lux HD (1987). Kinetics and selectivity of a low-voltage-activated calcium current in chick and rat sensory neurones. *J Physiol* **386**, 547–570.

Chapman ER (2002). Synaptotagmin: a Ca^{2+}-sensor that triggers exocytosis? *Nat Rev Mol Cell Biol* **3**, 498–508.

Charlton MP, Smith SJ & Zucker RS (1982). Role of presynaptic calcium ions and channels in synaptic facilitation and depression at the squid giant synapse. *J Physiol* **323**, 173–193.

Church PJ & Stanley EF (1996). Single L-type calcium channel conductance with physiological levels of calcium in chick ciliary ganglion neurons. *J Physiol* **496**, 59–68.

Colquhoun D (1971*a*). Fundamental operations and definitions. In *Lecture on Biostatistics*, ed. Colquhoun D, pp. 9–42. Clarendon Press, Oxford.

Colquhoun D (1971*b*). Stochastic (or random) processes. In *Lecture on Biostatistics*, ed. Colquhoun D, pp. 374–395. Clarendon Press, Oxford.

Datyner NB & Gage PW (1980). Phasic secretion of acetylcholine at a mammalian neuromuscular junction. *J Physiol* **303**, 299–314.

Dodge FA Jr & Rahamimoff R (1967). Co-operative action of calcium ions in transmitter release at the neuromuscular junction. *J Physiol* **193**, 419–432.

Dudel J (1981). The effect of reduced calcium on quantal unit current and release at the crayfish neuromuscular junction. *Pflugers Arch* **391**, 35–40.

Dudel J, Parnas H & Parnas I (1991). Evoked phasic release in frog nerve terminals obtained after block of Ca^{2+} entry by Cd^{2+}. *Pflugers Arch* **419**, 197–204.

Foster KA, Kreitzer AC & Regehr WG (2002). Interaction of postsynaptic receptor saturation with presynaptic mechanisms produces a reliable synapse. *Neuron* **36**, 1115–1126.

Hagiwara S & Byerly L (1981). Calcium channel. *Annu Rev Neurosci* **4**, 69–125.

Hoyle G & Wiersma CA (1958). Excitation at neuromuscular junctions in Crustacea. *J Physiol* **143**, 403–425.

Hua SY & Charlton MP (1999). Activity-dependent changes in partial VAMP complexes during neurotransmitter release. *Nat Neurosci* **2**, 1078–1083.

Hua SY, Teylan MA & Cimenser A (2007). An antibody to synaptotagmin I facilitates synaptic transmission. *Eur J Neurosci* **25**, 3217–3225.

Katz B & Miledi R (1965). The measurement of synaptic delay, and the time course of acetylcholine release at the neuromuscular junction. *Proc R Soc Lond B Biol Sci* **161**, 483–895.

Lin RC & Scheller RH (1997). Structural organization of the synaptic exocytosis core complex. *Neuron* **19**, 1087–1094.

Littleton JT, Stern M, Schulze K, Perin M & Bellen HJ (1993). Mutational analysis of *Drosophila* synaptotagmin demonstrates its essential role in Ca^{2+}-activated neurotransmitter release. *Cell* **74**, 1125–1134.

Llinás R, Steinberg IZ & Walton K (1976). Presynaptic calcium currents and their relation to synaptic transmission: voltage clamp study in squid giant synapse and theoretical model for the calcium gate. *Proc Natl Acad Sci U S A* **73**, 2918–2922.

Llinás R, Steinberg IZ & Walton K (1981). Relationship between presynaptic calcium current and postsynaptic potential in squid giant synapse. *Biophys J* **33**, 323–351.

Millar AG, Bradacs H, Charlton MP & Atwood HL (2002). Inverse relationship between release probability and readily releasable vesicles in depressing and facilitating synapses. *J Neurosci* **22**, 9661–9667.

Millar AG, Zucker RS, Ellis-Davies GC, Charlton MP & Atwood HL (2005). Calcium sensitivity of neurotransmitter release differs at phasic and tonic synapses. *J Neurosci* **25**, 3113–3125.

Millet O, Bernado P, Garcia I, Rizo J & Pons M (2002). NMR measurement of the off rate from the first calcium-binding site of the synaptotagmin I C2A domain. *FEBS Lett* **516**, 93–96.

Msghina M, Govind CK & Atwood HL (1998). Synaptic structure and transmitter release in crustacean phasic and tonic motor neurons. *J Neurosci* **18**, 1374–1382.

Parnas H, Hovav G & Parnas I (1989). Effect of Ca^{2+} diffusion on the time course of neurotransmitter release. *Biophys J* **55**, 859–874.

Sabatini BL & Regehr WG (1996). Timing of neurotransmission at fast synapses in the mammalian brain. *Nature* **384**, 170–172.

Schiavo G, Benfenati F, Poulain B, Rossetto O, Polverino de Laureto P, DasGupta BR & Montecucco C (1992). Tetanus and botulinum-B neurotoxins block neurotransmitter release by proteolytic cleavage of synaptobrevin. *Nature* **359**, 832–835.

Schneggenburger R, Meyer AC & Neher E (1999). Released fraction and total size of a pool of immediately available transmitter quanta at a calyx synapse. *Neuron* **23**, 399–409.

Schneggenburger R & Neher E (2000). Intracellular calcium dependence of transmitter release rates at a fast central synapse. *Nature* **406**, 889–893.

Shahrezaei V & Delaney KR (2004). Consequences of molecular-level Ca^{2+} channel and synaptic vesicle colocalization for the Ca^{2+} microdomain and neurotransmitter exocytosis: a monte carlo study. *Biophys J* **87**, 2352–2364.

Simon SM & Llinás RR (1985). Compartmentalization of the submembrane calcium activity during calcium influx and its significance in transmitter release. *Biophys J* **48**, 485–498.

Sollner TH (2003). Regulated exocytosis and SNARE function. *Mol Membr Biol* **20**, 209–220.

Sollner T, Whiteheart SW, Brunner M, Erdjument-Bromage H, Geromanos S, Tempst P & Rothman JE (1993). SNAP receptors implicated in vesicle targeting and fusion. *Nature* **362**, 318–324.

Waldeck RF, Pereda A & Faber DS (2000). Properties and plasticity of paired-pulse depression at a central synapse. *J Neurosci* **20**, 5312–5320.

Zucker RS & Stockbridge N (1983). Presynaptic calcium diffusion and the time courses of transmitter release and synaptic facilitation at the squid giant synapse. *J Neurosci* **3**, 1263–1269.

Acknowledgements

We thank Dr Peter Balsam for his constructive comments for this study. This work was supported by a Barnard start-up fund for S.-Y.H.